

NON-FERMI POWER LAW ACCELERATION IN ASTROPHYSICAL PLASMA SHOCKS

C. B. HEDEDAL¹, T. HAUGBØLLE¹, J. TRIER FREDERIKSEN², Å. NORDLUND¹

Draft version November 14, 2018

ABSTRACT

Collisionless plasma shock theory, which applies for example to the afterglow of gamma ray bursts, still contains key issues that are poorly understood. In this paper we study charged particle dynamics in a highly relativistic collisionless shock numerically using $\sim 10^9$ particles. We find a power law distribution of accelerated electrons, which upon detailed investigation turns out to originate from an acceleration mechanism that is decidedly different from Fermi acceleration. Electrons are accelerated by strong filamentation instabilities in the shocked interpenetrating plasmas and coincide spatially with the power law distributed current filamentary structures. These structures are an inevitable consequence of the now well established Weibel-like two-stream instability that operates in relativistic collisionless shocks. The electrons are accelerated and decelerated instantaneously and locally; a scenery that differs qualitatively from recursive acceleration mechanisms such as Fermi acceleration. The slopes of the electron distribution power laws are in concordance with the particle power law spectra inferred from observed afterglow synchrotron radiation in gamma ray bursts, and the mechanism can possibly explain more generally the origin of non-thermal radiation from shocked inter- and circum-stellar regions and from relativistic jets.

Subject headings: acceleration of particles — gamma rays: bursts — shock waves — instabilities — magnetic fields — supernova remnants

1. INTRODUCTION

Given the highly relativistic conditions in the outflow from gamma ray bursts (GRBs), the mean free path for particle Coulomb collisions in the afterglow shock is several orders of magnitude larger than the fireball itself. In explaining the microphysical processes that work to define the shock, MHD becomes inadequate and collisionless plasma shock theory stands imperative. In particular two key issues remain, namely the origin and nature of the magnetic field in the shocked region, and the mechanism by which electrons are accelerated from a thermal population to a power law distribution $N(\gamma)d\gamma \propto \gamma^{-p}$. Both ingredients are needed to explain the observed afterglow spectra (e.g. Kumar 2000; Panaitescu & Kumar 2001).

Regarding the origin of the magnetic field in the shocked region, observations are not compatible with a compressed inter-stellar magnetic field, which would be orders of magnitude smaller than needed (Gruzinov & Waxman 1999). It has been suggested that a Weibel-like two-stream instability can generate a magnetic field in the shocked region (Medvedev & Loeb 1999; Frederiksen et al. 2003; Nishikawa et al. 2003; Silva et al. 2003). Computer experiments by Frederiksen et al. (2004) showed that the nonlinear stage of a two-stream instability induces a magnetic field *in situ* with an energy content of a few percent of the equipartition value, consistent with that required by observations.

Fermi acceleration (Fermi 1949) has, so far, been widely accepted as the mechanism that provides the inferred electron acceleration. It has been employed extensively in Monte Carlo simulations (e.g. Niemiec & Ostrowski (2004) and references therein), where it operates in conjunction with certain assumptions about the scattering of particles and the structure

of the magnetic field. The mechanism has, however, not been conclusively demonstrated to occur in *ab initio* particle simulations. As pointed out by Niemiec & Ostrowski (2004), further significant advance in the study of relativistic shock particle acceleration is unlikely without understanding the detailed microphysics of collisionless shocks. Also, recently Baring & Braby (2004) found that particle distribution functions (PDFs) inferred from GRB observations are in contradistinction with standard acceleration mechanisms such as diffusive Fermi acceleration.

In this letter we study *ab initio* the particle dynamics in a collisionless shock with bulk Lorentz factor $\Gamma = 15$. We find a new particle acceleration mechanism, which we present in Section 2. Detailed numerical results are presented and interpreted in Section 3, while Section 4 contains the conclusions.

2. A NEW ACCELERATION MECHANISM

We have performed a series of numerical experiments where collisionless shocks are created by two colliding plasma populations. These experiments are described in more detail below, but a common feature is that the electron PDF has a high energy tail which is power law distributed. By carefully examining the paths of representative accelerated electrons, tracing them backwards and forwards in time, we have been able to identify the mechanism responsible for their acceleration. The acceleration mechanism, which as far as we can tell has not been discussed in the literature previously, works as follows:

When two non-magnetized collisionless plasma populations interpenetrate, current channels are formed through a Weibel-like two-stream instability (Medvedev & Loeb 1999; Frederiksen et al. 2003; Nishikawa et al. 2003; Silva et al. 2003). In the nonlinear stage of evolution of this instability, ion current channels merge into increasingly stronger patterns, while electrons act to Debye shield these channels, as shown by Frederiksen et al. (2004). That work further showed that a Fourier decomposition of the transverse ion current fil-

¹ Niels Bohr Institute for Astronomy, Physics, and Geophysics, Juliane Maries Vej 30, 2100 København Ø, Denmark

² Stockholm Observatory, Roslagstullbacken 21, 106 91 Stockholm, Sweden

Electronic address: hededal@astro.ku.dk

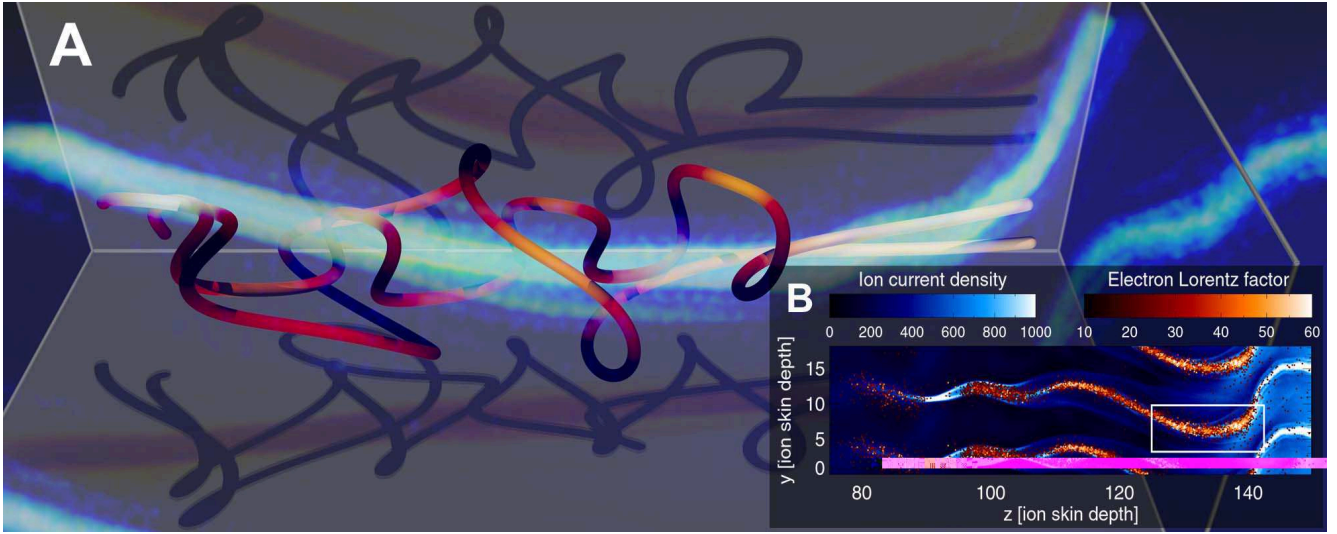


FIG. 1.— (A) Ray traced electron paths (red) and current density (blue). The colors of the electron paths reflect their four velocity according to the color table in the inset (B). The shadows are equivalent to the x and y projections of their paths. The ion current density is shown with blue colors according to the color table in the inset. The inset also shows the ion current density (blue) integrated along the x axis with the spatial distribution of fast moving electrons (red) over plotted.

aments exhibits power law behavior which has been recently confirmed by Medvedev et al. (2004).

At distances less than the Debye length, the ion current channels are surrounded by transverse electric fields that accelerate the electrons toward the current channels. However, the magnetic fields that are induced around the current channels act to deflect the path of the accelerated electrons, boosting them instead in the direction of the ion flow. Since the forces working are due to quasi-stationary fields the acceleration is a simple consequence of potential energy being converted into kinetic energy. Therefore the electrons are decelerated again when leaving the current channel, and reach their maximal velocities at the centers of the current channels. Hence, as illustrated by Fig. 1B, the spatial distribution of the high energy electrons is a direct match to the ion current channels and the properties of the accelerated electrons depend primarily on the local conditions in the plasma.

One might argue that the near-potential behavior of the electrons, where they essentially must lose most of their energy to escape from the current channels, would make the mechanism uninteresting as an acceleration mechanism since fast electrons cannot easily escape. However, this feature may instead be a major advantage, since it means that energy losses due to escape are small, and that the electrons remain trapped long enough to have time to lose their energy via a combination of bremsstrahlung and synchrotron or jitter radiation. We observe that only a very small fraction of the electrons manage to escape, while still retaining most of their kinetic energy. This happens mainly at sudden bends or mergers of the ion channels, where the electron orbits cannot be described in terms of a particle moving in a static electromagnetic field.

To analyze the acceleration scenario quantitatively we use the sketch in Fig. 2. We assume that the ion current channel has radius R , that the total charge inside the cylinder per unit length is λ and the ions stream with velocity u in the laboratory rest frame (see Fig. 2 and inset for definition of rest frames). Consider an electron with charge $-q$ and mass m at a distance r from the center of the channel, initially having no velocity components perpendicular to the cylinder. By

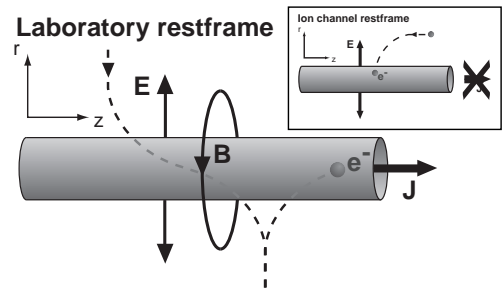


FIG. 2.— An ion current channel surrounded by an electric – and a magnetic field. Electrons in the vicinity of the current channels are thus subject to a Lorentz force with both an electric and magnetic component, working together to accelerate the electrons along the ion flow. Crossing the center of the channel the process reverses leading to an oscillating movement along the channel.

analyzing everything in the ion channel rest frame the problem reduces to electrostatics and it is possible to analytically calculate the change in four velocity of the electron when it reaches the surface of the cylinder. Since the electric force only works along the r -axis, the four velocity along the z -axis of the electron is conserved in the ion channel rest frame. Hence we can calculate both the total change in energy and the change in the different velocity components. Returning to the laboratory rest frame we find

$$\Delta\gamma_{electron} = \frac{q\lambda}{2\pi mc^2 \epsilon_0} \ln \frac{r}{R} \quad (1)$$

$$\Delta(\gamma v_z)_{electron} = u \Delta\gamma_{electron}. \quad (2)$$

The change in the Lorentz boost is directly proportional to the total charge inside the channel and inversely proportional to the electron mass. Debye shielding reduces the electric field further away from the ion channel, so the estimate above is only valid for distances smaller than a Debye length.

3. COMPUTER EXPERIMENTS

The experiments were performed with the three dimensional relativistic kinetic and electromagnetic particle-in-cell

code described by Frederiksen et al. (2004). The code works from first principles, by solving Maxwell's equations for the electromagnetic fields and solving the Lorentz force equation of motion for the particles.

Two colliding plasma populations are set up in the rest frame of one of the populations (downstream, e.g. a jet). A less dense population (upstream, e.g. the ISM) is continuously injected at the left boundary with a relativistic velocity corresponding to a Lorentz factor $\Gamma = 15$. The two populations initially differ in density by a factor of 3. We use a computational box with $125 \times 125 \times 2000$ grid points and a total of 8×10^8 particles. The ion rest frame plasma frequency in the downstream medium is $\omega_{pi} = 0.075$, rendering the box 150 ion skin depths long. The electron rest frame plasma frequency is $\omega_{pe} = 0.3$ in order to resolve also the microphysics of the electrons. Hence the ion-to-electron mass ratio is $m_i/m_e = 16$. Other mass ratios and plasma frequencies were used in complementary experiments. Initially, both plasma populations are unmagnetized.

The maximum experiment duration has $t_{max} = 340 \omega_{pi}^{-1}$, which is sufficient for the continuously injected upstream plasma ($\Gamma = 15$, $v \sim c$) to travel 2.3 times the length of the box. The extended size and duration of these experiments enable observations of the streaming instabilities and concurrent particle acceleration through several stages of development (Frederiksen et al. 2004). Momentum losses to radiation (cooling) are presently not included in the model. We have, however, verified that none of the accelerated particles in the experiment would be subject to significant synchrotron cooling. The emitted radiation may thus be expected to accurately reflect the distribution of accelerated electrons.

When comparing numerical data with Eq. 1 we take r to be the radius where Debye shielding starts to be important. Using a cross section approximately in the middle of Fig. 1 we find $\Delta(\gamma v_z)_{electron} = 58 \ln(r/R)$. It is hard to determine exactly when Debye shielding becomes effective, but looking at electron paths and the profile of the electric field we estimate that $\ln(r/R) \approx 1.3$. Consequently, according to Eq. 1, the maximally attainable four velocity in this experiment is in the neighborhood of $(\gamma v_z)_{max} = 75$. This is in good agreement with the results from our experiments, where the maximum four velocity is $(\gamma v_z)_{max} \simeq 80$.

The theoretical model does of course not cover all details of the experiment. For example, in general the electrons also have velocity components parallel to the magnetic field; instead of making one dimensional harmonic oscillations in the plane perpendicular to the current channel the electrons will describe ellipsoidal paths. Fig. 1 shows the path of two electrons in the vicinity of an ion channel. But, overall, the electrons behave as expected from the model considerations. Consequently, high speed electrons are tightly coupled to the ion channels, as clearly illustrated by Fig. 1B.

Figure 4 shows that the electrons are power law distributed at high energies, with index $p = 2.7$. The electrons at the high gamma cutoff are found where the ion current peaks, as may be seen from Fig. 3. The maximum ion current is limited by the size of our box; larger values would probably be found if the merging of current channels could be followed further down stream. The PDF is not isotropic in any frame of reference due to the high anisotropy of the Weibel generated electromagnetic field. The power law in the electron PDF is dominant for $10 < \gamma < 30$. Likewise, a power law dominates the ion current channel strength, J_{ion} , for $100 < J_{ion} < 1000$ (inset). A relation between the power law distributions of

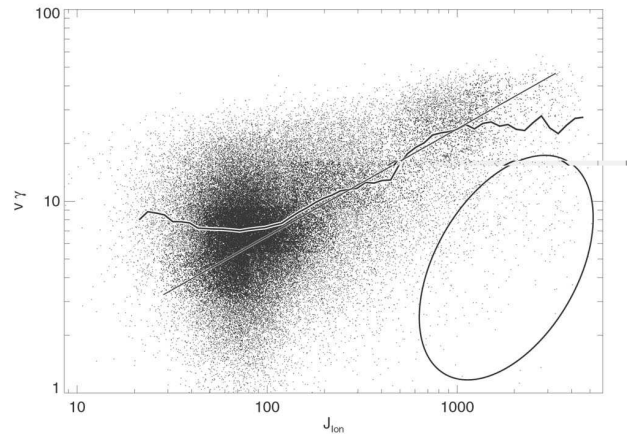


FIG. 3.— A scatter plot of the local ion current density J_{ion} versus the four velocity of the electrons in a region downstream of the shock. Overplotted is a line (thin) showing the average four velocity as a function of J_{ion} , and a line (thick) showing a straight line fit. Because 'cold' trapped thermal electrons (indicated with the ellipse) exist inside the ion current channel they count towards lowering the average four velocity at high J_{ion} . If we cleaned our scatter plot, statistically removing all thermal electrons we would see a much tighter relation. Such cleaning, though, is rather delicate and could introduce biases by itself. The trend is clearly there though even for the 'raw' data.

these two quantities on their respective intervals is provided with Fig. 3: We see that the average four velocity is proportional (straight line fit) to a power of the local ion current density on their respective relevant intervals, $10 < \gamma < 30$ and $100 < J_{ion} < 1000$. Their kinship stems from the fact that acceleration is local. J_{ion} has a power law tail and its potential drives the high energy distribution of the electrons according to Eq. 1, thus forming a power law distributed electron PDF.

Measuring the rate at which the in-streaming ions transfer momentum to the ion population initially at rest allows us to make a crude estimate of the length scales over which the two-stream instability in the current experiment would saturate due to ion thermalization. A reasonable estimate appears to be approximately 10 times the length of the current computational box, or about 1500 ion skin depths. Assuming that the shock propagates in an interstellar environment with a plasma density of $\sim 10^6 \text{ m}^{-3}$ we may calculate a typical ion skin depth. Comparing this value with the upstream ion skin depth from our experiments, we find that the computational box corresponds to a scale of the order of 10^7 m , or equivalently that the collisionless shock transition region of the current experiment corresponds to about 10^8 m . For an ion with a Lorentz factor $\gamma = 15$ this length corresponds roughly to 40 ion gyro radii in the average strength of the generated magnetic field. But we stress that the in-streaming ions actually do not really gyrate since they mainly travel inside the ion current channels where the magnetic field, by symmetry, is close to zero. Also, the strong electromagnetic fields generated by the Weibel instability and the non-thermal electron acceleration, which is crucial for the interpretation of GRB afterglow observations, emphasize the shortcoming of MHD in the context of collisionless shocks.

In the computer experiments presented here we have used an mass ratio $m_i/m_e = 16$ in order to resolve the dynamics of both species. Eq. 1 suggests that reducing the electron mass to $1/1836 m_i$ will increase the acceleration of the electrons to maximum energies in the neighborhood of 5 GeV. Even

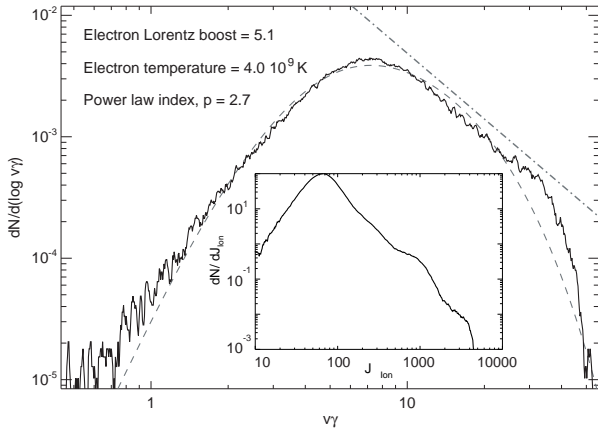


FIG. 4.— The normalized electron particle distribution function downstream of the shock. The dot-dashed line is a power law fit to the non-thermal high energy tail, while the dashed curve is a Lorentz boosted thermal electron population. The histogram is made from the four velocities of electrons in a thin slice in the z -direction of the computational box. The inset shows a similar histogram for ion current density sampled in each grid point in the same slice. The bump in the inset is a statistical fluctuation due to a single ion channel.

further acceleration may occur as ion channels keep growing down stream, outside of our computational box.

The scaling estimates above depend, among other things, on plasma densities, the bulk Lorentz factor, and the mass ratio (m_i/m_e). A parameter study is necessary to explore these dependencies, but this is beyond the scope of the present paper. We thus stress that the extrapolations performed here are speculative and that unresolved physics could influence the late stages of the instability in new and interesting ways.

When the in-streaming ions are fully thermalized they can no longer support the magnetic field structures. Thus one might speculate that the radiating region of the GRB afterglow is actually very thin, as suggested by Rossi & Rees (2003). Further, traditional synchrotron radiation theory does not apply to intermittent magnetic field generated by the two-stream instability, since the electron gyro radii often are larger than the scales of the magnetic field structures. We emphasize the importance of the theory of jitter radiation (Medvedev 2000).

4. CONCLUSIONS

We have proposed a new acceleration mechanism for electrons in collisionless shocks. The theoretical considerations were suggested by particle-in-cell computer experiments,

which also allowed quantitative comparisons with the theoretical predictions. We have shown that the non-thermal acceleration of electrons is directly related to the ion current channels in the shock transition zone. The results are applicable to interactions between relativistic outflows and the interstellar medium. Such relativistic outflows occur in GRB afterglows and in jets from compact objects (Fender et al. 2004). The suggested acceleration scenario might overcome some of the problems pointed out by Baring & Braby (2004) regarding the apparent contradiction between standard Fermi acceleration and spectral observations of GRBs.

The mechanism has important implications for the way we understand and interpret observations of collisionless shocks:

1. The acceleration mechanism is capable of creating a power law electron distribution in a collisionless shocked region. In the computer experiment presented here a bulk flow with $\Gamma = 15$ results in a power law slope $p = 2.7$ for the electron PDF. Additional experiments will be needed to disentangle what determines the exact value of the slope.

2. The acceleration is local; electrons are accelerated to a power law in situ. Therefore the observed radiation field may be tied directly to the local conditions of the plasma and could be a strong handle on the physical processes.

3. Our results strengthen the point already made by Frederiksen et al. (2004); that the fractions of the bulk kinetic energy that go into the electrons and the magnetic field, ϵ_e and ϵ_B respectively, are not free and independent parameters of collisionless shock theory. Most likely they represent interconnected parts of the same process.

4. In the case of a weak or no upstream magnetic field, the Weibel-like two-stream instability is able to provide the necessary electromagnetic fields. We have shown here that the collisionless shocked region is relatively thin, and we suggest that the non-thermal radiation observed from GRB afterglows and relativistic jets in general is emitted from such a relatively thin shell.

It is clear that the non-thermal electron acceleration, the ion current filamentation, the magnetic field amplification/generation, and hence the strong non-thermal radiation from the shock, is beyond the reach of MHD to explain. Whether the relativistic MHD jump conditions become valid on any larger scale is not possible to decide from the simulations presented in this paper.

We thank the Danish Center for Scientific Computing for granting the computer resources that made this work possible. The authors will also like to thank Ken-Ichi Nishikawa, Mikhail Medvedev and the referee for their comments and suggestions. The work of ÅN was supported by a grant from the Danish Natural Science Research Council.

REFERENCES

- Baring, M. G., & Braby, M. L. 2004, *ApJ*, 613, 460
 Fender, R., Wu, K., Johnston, H., Tzioumis, T., Jonker, P., Spencer, R., & van der Klis, M. 2004, *Nature*, 427, 222
 Fermi, E. 1949, *Physical Review*, 75, 1169
 Frederiksen, J. T., Hededal, C. B., Haugbølle, T., & Nordlund, Å. 2003, *Proceedings of the 2002 Niels Bohr Summer Institute*, ArXiv Astrophysics e-prints, astro-ph/0303360
 Frederiksen, J. T., Hededal, C. B., Haugbølle, T., & Nordlund, Å. 2004, *ApJ*, 608, L13
 Gruzinov, A., & Waxman, E. 1999, *ApJ*, 511, 852
 Kumar, P. 2000, *ApJ*, 538, L125
 Medvedev, M. V. 2000, *ApJ*, 540, 704
 Medvedev, M. V., Fiore, M., Fonseca, R., Silva, L., & Mori, W. 2004, submitted to *ApJ*, astro-ph/0409382
 Medvedev, M. V., & Loeb, A. 1999, *ApJ*, 526, 697
 Niemiec, J., & Ostrowski, M. 2004, *ApJ*, 610, 851
 Nishikawa, K.-I., Hardee, P., Richardson, G., Preece, R., Sol, H., & Fishman, G. J. 2003, *ApJ*, 595, 555
 Panaitescu, A., & Kumar, P. 2001, *ApJ*, 560, L49
 Rossi, E., & Rees, M. J. 2003, *MNRAS*, 339, 881
 Silva, L. O., Fonseca, R. A., Tonge, J. W., Dawson, J. M., Mori, W. B., & Medvedev, M. V. 2003, *ApJ*, 596, L121